Exploring nanoscale electrical and electronic properties of organic and polymeric functional materials by atomic force microscopy based approaches

Vincenzo Palermo,[a] Andrea Liscio,[a] Matteo Palma,[b] Mathieu Surin,[bc] Roberto Lazzaroni[c] and Paolo Samorì*[ab]

Received (in Cambridge, UK) 23rd January 2007, Accepted 9th March 2007
First published as an Advance Article on the web 30th March 2007
DOI: 10.1039/b701015j

Beyond imaging, atomic force microscopy (AFM) based methodologies enable the quantitative investigation of a variety of physico-chemical properties of (multicomponent) materials with a spatial resolution of a few nanometers. This Feature Article is focused on two AFM modes, *i.e.* conducting and Kelvin probe force microscopies, which allow the study of electrical and electronic properties of organic thin films, respectively. These nanotools provide a wealth of information on (dynamic) characteristics of tailor-made functional architectures, opening pathways towards their technological application in electronics, catalysis and medicine.

Introduction

Making use of nature as a source of inspiration, hierarchical self-assembly provides tools for bottom-up construction of sophisticated functional nanoscale architectures,[1] thus paving the route towards their optimization for application in a variety of fields including sensors, catalysis and electronics.[2,3] Since the characteristics of molecular materials are known to depend on their shape and size[4] as well as on the order at the supramolecular level,[5,6] it is crucial to be able to unveil (dynamic) properties of nanoscale architectures. Among the different properties of materials, the electrical and electronic properties are widely exploited in sensor as well as in organic opto- and nano-electronic technologies.

Scanning probe microscopies (SPMs) are very powerful tools, which make it possible to explore, in a non-invasive manner, (supra)molecular architectures across a wide range of length scales, even down to the nanoscale. Moreover, SPM investigations can be carried out under different environmental conditions, thereby enabling the exploration of complex systems in their native environments. Simultaneously to morphological and structural characterizations, many (dynamic) physico-chemical properties can be studied using these tools,

[a]*Istituto per la Sintesi Organica e la Fotoreattività, Consiglio Nazionale delle Ricerche (C.N.R.), via Gobetti 101, I-40129 Bologna, Italy. E-mail: samori@isis-ulp.org; Fax: +33-3-90245161; Tel: +33-3-90245160*
[b]*Nanochemistry Laboratory, ISIS/CNRS UMR 7006, Université Louis Pasteur, 8, allée Gaspard Monge, F-67083 Strasbourg, France*
[c]*Chimie des Matériaux Nouveaux, Université de Mons-Hainaut, 20, Place du Parc, B-7000 Mons, Belgium*

Vincenzo Palermo

Vincenzo Palermo (S. Severo, Italy, 1972) obtained his Laurea in Industrial Chemistry at the University of Bologna. He performed his PhD at the Institute for the Organic Synthesis and Photoreactivity of the National Research Council (ISOF-CNR), Italy, working on STM characterization of silicon nanostructures for microelectronics. He worked in the groups of Prof. Y. K. Levine (University of Utrecht, The Netherlands) and Prof. R. A. Wolkow (National Research Council, Canada). His main research interests involve the structural and electronic characterization of organic semiconductor nanostructures using scanning probe microscopies. His work has been awarded with the graduate student award at EMRS (2003) and by the Italian Society for Microscopic Sciences (SISM) award 2006. He is presently a research scientist at ISOF-CNR.

Andrea Liscio

Andrea Liscio was born in Roma (Italy) in 1975. He received his ''Laurea'' in Physics from the University of Roma 3 in 2000. He performed his PhD (2004) at the Institute of Inorganic Methodologies and Plasmas of the National Research Council (IMIP-CNR), Italy, modelling electron–surface interactions to study surface and interface electronic systems using electronic spectroscopies. His current research interests include the morphological and electrical characterization of thin films and supramolecular assemblies for optoelectronics using scanning-probe techniques. In 2005 he started postdoctoral research at the Institute for the Organic Synthesis and Photoreactivity of the National Research Council (ISOF-CNR).

such as mechanical,[7] magnetic and electronic properties.[8–10] In this way a correlation between these measured characteristics and the structure becomes possible. The acquired knowledge is therefore fundamental for the optimization of molecular materials and devices.

Among the different SPMs, atomic force microscopy (AFM)[11–13] is undoubtedly the most versatile set-up as it enables the investigation of both electrically conducting and insulating molecular assemblies. Different AFM modifications have been introduced over the past decade aiming at studying various properties of nanostructures.[14–20]

In this Feature Article, we focus on two AFM-based methodologies, namely conducting and Kelvin probe force microscopies, which can be used to investigate, under ambient atmosphere, the electrical and electronic properties of organic nanostructures of potential interest in the field of nanoelectronics and more generally in nanotechnology.

Conducting probe AFM on organic thin films

Different approaches and junction configurations have been proposed and employed to study the charge transport properties of organic nanostructures, including those based on either one or two mercury-drops,[21] nanopores,[22] break junctions,[23] facing Au nanoelectrodes[24] also assisted by metallic nanoparticles,[25,26] and by using scanning probe microscopies (SPMs). Among SPMs, scanning tunneling microscopy (STM) and spectroscopy as well as conducting probe atomic force

Matteo Palma

Matteo Palma (Roma, Italy, 1979) obtained his Laurea in Chemistry at the University of Rome, La Sapienza (Italy) with an experimental thesis on ''Self-assembly and electrical properties of π-conjugated supramolecular architectures'', performed under the supervision of Dr Paolo Samorì at the ISOF-CNR, Bologna (Italy). In 2004, he started his PhD in Dr Paolo Samorì's group at the Institut de Science et d'Ingénierie Supramoléculaires of the Université Louis Pasteur of Strasbourg (ISIS-ULP), France, within the Marie Curie EST project ''SUPER'' (Supramolecular Devices at Surfaces). His current research is focused in particular on the development of prototypes of supramolecular wires at surfaces. His work has been awarded the young scientist award at EMRS (2006).

Mathieu Surin

Mathieu Surin (Mons, Belgium, 1979) obtained his PhD from the University of Mons-Hainaut in 2005, working in the field of conjugated (co)polymers with Prof. Roberto Lazzaroni. In 2005 he was invited as a researcher at UC-Santa Barbara, working under the supervision of Prof. Alan Heeger. He then did a post-doctoral stay at the 'Institut de Science et d'Ingénierie Supramoléculaires' at Strasbourg in the lab of Prof. Paolo Samorì. Since 2007 he is 'Chargé de Recherches' of the FNRS-Belgium. His main research interests are the field of supramolecular chemistry and the understanding of morphology–property relationships, using tools such as scanning probe microscopies and molecular modeling.

Roberto Lazzaroni

Roberto Lazzaroni obtained a PhD in Chemistry from the University of Namur (Belgium) in 1987. He joined the group of J. L. Brédas at the University of Mons-Hainaut in 1990, as a research associate of the Belgian National Science Foundation (FNRS). He became research director of FNRS in 2001 and joined the faculty in Mons in 2003. His main research interests are the supramolecular organisation in conjugated materials, the relationship between such organisation and the electronic and optical properties, and the microscopic morphology of thin films of complex polymer materials.

Paolo Samorì

Paolo Samorì (Imola, Italy, 1971) obtained a Laurea (master's degree) in Industrial Chemistry at University of Bologna in 1995. He took his PhD in 2000 in Prof. Jürgen P Rabe's group (Humboldt University Berlin) on self-assembly of conjugated (macro)molecules at surfaces. After a Postdoc in the same lab he was appointed, in 2001, Research Scientist at the Institute for the Organic Synthesis and Photoreactivity of the National Research Council (ISOF-CNR), Italy. From 2003 he has been invited to hold a Visiting Professorship at the Institut de Science et d'Ingénierie Supramoléculaires of Université Louis Pasteur of Strasbourg (ISIS-ULP), France where he is Director of the Nanochemistry Laboratory. His current research interests include the applications of scanning probe microscopies beyond imaging, hierarchical self-assembly of hybrid architectures at surfaces, supramolecular electronics, and the fabrication of molecular-scale nanodevices. His work has been awarded various prizes, including the young scientist awards at EMRS (1998) and MRS (2000) as well as the IUPAC Prize for Young Chemists 2001 and the Vincenzo Caglioti award 2006 granted by the Accademia Nazionale dei Lincei (Italy).

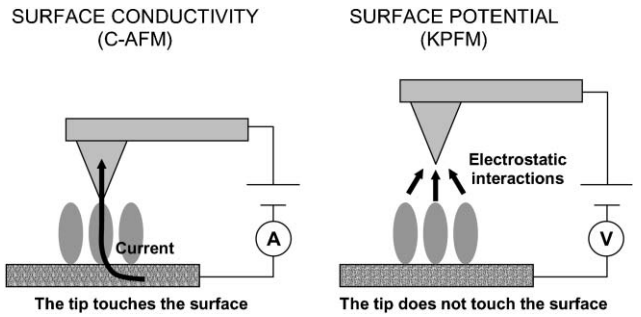

Scheme 1 Experimental set-up for conducting AFM and Kelvin probe force microscopy. See text for details.

microscopy have proven to be efficient tools to unravel simultaneously electrical and structural properties of nanostructures. The main advantage of conducting probe atomic force microscopy, also known as conductive AFM (hereafter named C-AFM), consists in the possibility to simultaneously perform topographical and electrical characterizations. This technique relies on the use of an electrically conducting AFM tip as one electrode and a conductive substrate, or patterned metallic electrode at surfaces, acting as counter electrode. When a voltage, typically lower than 10 volts, is applied between the two electrodes, a current usually ranging from a few fA to several μA can be measured with C-AFM (Scheme 1). The electrical current can be detected at a controlled voltage between the tip and the metal electrode, either recording images, that can be used as a measure of the local conductivity, or collecting current–voltage (*I–V*) and current–vertical distance (*I–Z*) curves.[27–30] In order to obtain *I–V* characteristics of defined nano-objects at surfaces, 'point-contact' measurements at given locations of the sample surface can be recorded with the tip held fixed while the tip–sample bias is ramped. On the other hand, for *I–Z* measurements, the sample bias is kept constant while the scanner is moved along the *Z* direction, perpendicular to the sample surface. In fact, C-AFM exploits the conventional positioning scheme of the tip *via* the force detection of AFM. Being decoupled from the current signal, it permits the recording of simultaneous topographic and current features. Notably, this differs from STM: in this latter technique, the positioning of the tip is achieved *via* the tunnel current detection, often making the control of the tip–sample distance quite delicate. Moreover, while STM can only probe conducting materials or ultra-thin insulating films supported on conductive substrates, C-AFM is much more versatile since it can be employed to characterize insulating materials in thin films, *e.g.*, silicon oxide, alkane layers, and self-assembled monolayers (SAMs) on conducting surfaces, or relatively resistive materials such as organic semiconductors.[29–32] The lateral resolution of C-AFM is not limited by the prime physical properties employed to map the surface (*i.e.* electron transport) – in contrast to Kelvin probe force microscopy (see below) – but rather by the probe radius of commercially available conducting probes, *i.e.* typically of a few nm up to ten nm. Regarding this issue, STM offers a better lateral resolution, being on the sub-nm range. Albeit C-AFM has been employed to study the electrical properties of a large variety of materials, here we mostly highlight studies focused on the characterization of organic nanostructures and thin layers.

C-AFM can be employed in two different configurations: *horizontal* and *vertical*. In both cases, the C-AFM tip acts as one electrode. In the *horizontal* configuration, the electrically active material is supported on an insulating surface (*e.g.*, SiO_2) and it is connected to one patterned electrode. In the *vertical* configuration, a (mono)layer of the material is deposited on a conductive surface (acting as counter electrode) and the tip is placed on top of the layer.

Horizontal configuration

The development of C-AFM contributed to explore the electronic properties of carbon nanotubes, in an effort towards a more comprehensive understanding of charge transport in such systems. This was accomplished by studying the resistivity of individual multi-wall carbon nanotubes positioned between gold electrodes supported on a SiO_2 substrate, using the C-AFM probe as the counter electrode. In this way the topography and the resistance of the nanostructure were mapped simultaneously.[28] It was observed that curved nanotubes (*i.e.*, possessing structural defects) exhibit a resistivity almost one order of magnitude higher than that of straight carbon nanotubes. In a similar way, ion beams have been employed to generate defects in single walled carbon nanotubes (SWCNTs). The induced change in charge transport properties has been probed by C-AFM. This result opened new paths towards the fine tuning of the electronic properties of such architectures.[33] It is worth noting that such experiments were carried out in contact mode. However, this mode is known to be too invasive to study relatively soft materials based on organic molecules and polymers. One way to minimize the load exerted by the tip on the sample, and therefore to avoid sample damage, is to explore its topography by dynamic, intermittent contact modes (*e.g.*, tapping-mode), and then perform stationary point-contact *I–V* experiments at given locations. This methodology has been used by Frisbie and co-workers to establish relationships between the morphology and the electrical properties of organic semiconducting architectures at the nanoscale. They studied sexithiophene (6T) crystals vacuum grown on a SiO_2 substrate and connected to a Au wire counter electrode (see Fig. 1(A)). *I–V* curves were recorded using a Au-coated tip at different tip–electrode horizontal distances (points 1–4 in Fig. 1(B)).[31] By measuring *I–V* curves at different locations, they estimated the 'contact resistance' by extrapolation at a zero tip–electrode distance. This allowed them to unravel the effect of a grain boundary in the crystal, as observed in the topography image between locations 1 and 2 in Fig. 1(B). A very high resistance was attributed to the grain boundary: for location 1 the resistance was found to be on the order of a few tens of MΩ, while on the opposite side of the grain boundary (points 2–4 in Fig. 1(B)) the resistance was about a few hundreds of GΩ. A linear extrapolation led to a contact resistance of 25 GΩ (see Fig. 1(D)), almost completely attributable to the grain boundary. This approach has also been applied to determine the effect of iodine doping of 6T thin films,[34] and to determine the conductance of single

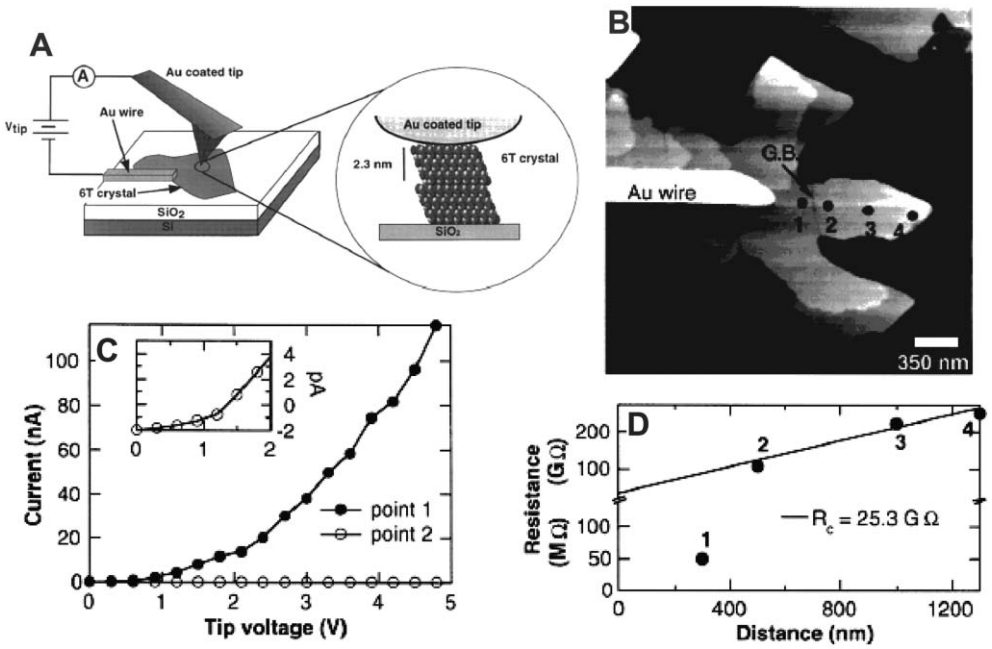

Fig. 1 (A) Scheme of the experimental set-up. (B) Topographic image of a sexithiophene (6T) crystal connected to a microfabricated Au wire on SiO_2. Two grain boundaries (GBs) are indicated with arrows. Point-contact measurements were made at points 1–4. The image was obtained in tapping-mode AFM with a Au-coated probe. (C) Point contact *I–V* characteristics obtained by C-AFM at points 1 and 2 labelled in (B). The inset shows an expanded view of the *I–V* trace at point 2. (D) Resistance (reciprocal of *I–V* slope at 5 V) *vs.* probe–wire separation distance. The linear fit through points 2, 3 and 4 has been used to estimate the GB resistance. Note the change of scale on the resistance axis. Reproduced with permission from ref. 31. Copyright 1999, Wiley–VCH.

oligo(*para*-phenylene vinylene) molecules through different nanosized gaps.[35]

Another way to study the electrical transport through organic semiconductors is to exploit field-effect transistor (FET) configurations with variable channel lengths, where the C-AFM probe and one metallic electrode serve as source and drain electrodes, respectively.[36] Such a set-up was also exploited to study copper phthalocyanine nano-crystals and to estimate the charge carrier mobility of single crystals.[37] Other SPM techniques such as tapping-mode AFM and electrostatic force microscopy have been employed in complementary approaches to study the relationship between the charge transport properties and the microscopic morphology of organic semiconductors within the channel of FETs.[38,39]

Vertical configuration

A key advantage of vertical contact C-AFM is the possibility of tailoring a metal–molecule–metal junction avoiding expensive top-down micro- or nanofabrication. The vertical contact configuration is well suited to study self-assembled monolayers (SAMs) on conductive surfaces,[40] such as thiolated molecules chemisorbed on Au or Ag substrates forming one-molecule-thick crystalline films. In particular this configuration has been employed to investigate a large variety of sulfur-terminated alkyl and aromatic molecules chemisorbed on gold[32] proving to be a useful tool to better understand the charge transport mechanisms through single molecules. The effects of tip load on the measured resistance, as well as substrate roughness, tip functionalization and chain length, have been thoroughly investigated. It is generally accepted that tunneling is the dominant mechanism for charge transport through organic monolayers in such a configuration, although the details of this mechanism are still not fully understood.[32,41] The tunneling through a series of SAMs (both alkylated and aromatic) has been explored in this way, leading to the determination of the tunneling decay parameter β.[32,42,43] According to the ballistic tunneling approximation, the linear conductance through an electrode–molecule–electrode is proportional to a transmission function T, reflecting the efficiency of the charge transport (across the contacts and through the molecule). β is related the efficiency of the tunneling through the molecule as eqn (1):[32]

$$T_{\mathrm{mol}} = \exp(-\beta l) \quad (1)$$

where T_{mol} is the transmission function of the charge through the molecule and l is the width of the barrier. β is indeed a function of the barrier height, *i.e.* the relative energies of the frontier molecular orbitals of the molecule and the Fermi level of the electrodes. For aliphatic chains, values of β were found to be around 0.6–1 $\mathrm{Å}^{-1}$, while for oligo(phenylene) chains it is estimated to lie in the 0.2–0.6 $\mathrm{Å}^{-1}$ range.[32] Noteworthy, these values are in agreement with those obtained by Hg drop junction investigations.[41] The difference in β values between aliphatic and aromatic systems is due to the smaller HOMO–LUMO gap for the latter ($\sim$3 eV *vs.* $\sim$8 eV for saturated hydrocarbons), leading to a higher tunneling efficiency for π-conjugated systems (or even the possibility of hopping charge transport to take place). The β value was also determined for alkanedithiols chemisorbed to the AFM tip,

by repeated formation of molecular junctions, with a value β around 1 (per carbon atom), *i.e.* very close to that determined by C-AFM for alkanethiols.[44] Moreover, when the molecule was covalently linked to both the substrate and the tip, the so formed contact exhibited a lower resistance when compared to the case of the molecule chemically-bonded only to the substrate.[45] This demonstrates that measurements of the intrinsic molecular properties require chemical bonds to both electrodes. This was accomplished binding a 1,8-octanedithiol molecule on one side to a gold substrate and on the other side to a gold nanoparticle which in turn was contacted to the C-AFM tip.[45] The use of such a small metallic nanocluster physically contacted to the tip allowed the control of the size of the molecule–tip junction, thus the number of molecules that are wired in a given measurement.

C-AFM has also shown its reliability to probe the potential of molecules as 'molecular wires'. Lindsay and co-workers used C-AFM in its vertical configuration to determine the electrical properties of single carotenoid molecules embedded in an insulating *n*-alkanethiol matrix (Fig. 2)[46] Such a study showed that a carotenethiol molecule can act, to a first approximation, as a ohmic resistor with a conductivity that is over a million times higher than an alkane chain of similar length. In addition, organometallic molecular wires have been recently studied by Chen *et al*. through an elegant description of pentachromium-oligo-α-pyridylamine switching strings chemisorbed between the C-AFM tip and a metallic substrate.[47] However, making use of this approach the isolation of single molecules is still a challenge since AFM imaging does not permit the unambiguous differentiation between a single molecule and an assembly of molecules embedded in the junction.

Additionally, C-AFM has been employed to study different molecular systems of biological interest. The electronic properties as a function of protein conformation have been explored by tuning the applied force and the tip bias on a metallo-protein chemisorbed to a metallic C-AFM tip.[48] The modulation of the barrier height and length by the imposed tip load has been studied and related to the protein conformation, in combination with molecular dynamics simulations.[48] Furthermore, C-AFM has been recently employed by different groups to study the charge transport of nucleotide-based architectures, including DNA, further fueling a debate that lies outside of the framework of this review.[49,50]

Junction fabrication by C-AFM, either in a vertical or horizontal configuration, has an additional important advantage as different conducting films can be coated to an AFM tip, offering the opportunity to easily examine the role of the contact material on the electrical behaviour of the junction. In this context different materials have been employed as conducting probes, including doped-silicon tips, Ag-, Au-, Pt- and Ti-coated tips as well as B-doped diamond films,[51] and chemically functionalized tips.[52] Taking into account primarily the sharpness and the electrical conductivity, diamond tips were found to be the most appropriate for conductivity measurements on SiO_2[30] while Au coated tips have been usually employed on organic materials, mainly because of their ability to chemisorb thiol-funtionalized molecules and because of the high work function of Au that can in principle facilitate low resistance contacts for π-conjugated organic systems having a low-lying HOMO (*i.e.* close to the work function of Au, around 5.1 eV).[31,32] Another important issue that has to be considered when performing C-AFM experiments is the interaction between the conducting probe and the sample surface: during *I–V* measurements there is a small "electrostatic load" on the junction in addition to the mechanical load applied by the cantilever.[43] Experiments carried out in air, in inert gas environments and in low polar solvents highlighted the effects of such a bias dependent adhesion force as well as a repulsive electrostatic interaction between the charged AFM probe and the contact-induced charge on an organic monolayer.[53,54]

Overall C-AFM has proven to be a powerful tool for electrical characterization of organic architectures, mainly because of the combination of high spatial resolution imaging and electrical measurements at given locations of the sample surface. Many factors have to be taken into account when performing such experiments, and future challenges should surely be addressed towards a better understanding and

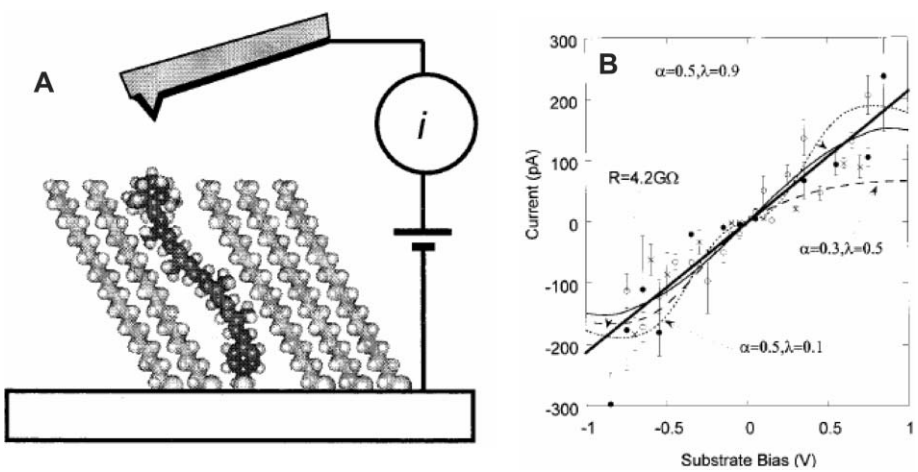

Fig. 2 (A) Scheme of the experimental set-up. (B) Current *vs*. substrate bias for three different sample preparations of carotene in an alkanethiol SAM. Contact forces are 3 nN (○ and ×) and 8.5 nN (●). The thick solid line is a best fit to a simple ohmic model (see ref. 46 for more details). Reproduced with permission from ref. 46. Copyright 1999, American Chemical Society.

quantification of the so obtained data. For instance, additional understanding can be obtained performing studies of *I–V* properties of nanostructures using different types of electrode pairs.

Kelvin probe force microscopy investigations

Among all the different characteristics of functional materials, their electronic properties are the subject of major interest and studies in view of their widespread exploitation in micro- and opto-electronics. For the specific case of organic materials, the density of electronic states strongly influences various properties such as conductivity, photoluminescence and charge mobility. Since this distribution is controlled both by the primary molecular structure and by supramolecular interactions, it is important to measure and correlate the morphology and the electric potential of a material on nanometric scales. Both Kelvin probe force microscopy (KPFM) and its simpler analogue electrostatic force microscopy (EFM) allow the mapping of a surface across a wide range of length scales with a lateral resolution of a few nm and a potential resolution of a few mV. In KPFM (also known as KPM or SKPM), a conductive tip scans over the surface interacting electrostatically with the surface under investigation (Scheme 1). An electronic feedback is used to match the potential of the tip to that of the material under investigation. When the potential of the tip exactly matches that of the material, the tip–sample electrostatic interaction is nullified. Under such condition, the potential of the material under study can be obtained from the voltage applied to the tip.

If compared to other SPMs (such as C-AFM), the main advantage of KPFM is that it is contact-less, which is an important feature especially for studies of both soft organic and biological samples. Furthermore, differently from C-AFM no charges are injected during the measurements and therefore KPFM measurements of working devices such as solar cells or thin film transistors can be performed without perturbing the operating device. We recently reported an extensive review on the applications of KPFM on organic materials.[55] Here we focus in more detail on the potential of KPFM to study dynamic physico-chemical properties and processes in very thin and nanostructured organic layers, including the electronic potential of well-defined molecular architectures at surfaces, and the changes in this potential due to chemical and electronic processes.[56]

Measuring the work function on nanometric scales

Typically, KPFM microscopy is employed to measure the local contact potential difference (CPD) between a conductive tip and a conductive sample. In this case the CPD corresponds to tip–sample work function difference, given that the work function (WF) of a solid is defined as the minimum energy required to remove an electron from the interior of the solid into vacuum, *i.e.* the energy difference between the vacuum level and either the Fermi level, in the case of a metal, or the most loosely bound electrons for a semiconductor or an insulating material.[57] A contact potential analysis performed by KPFM is a powerful way to cast light onto the electronic structures of a functional material. For a molecular assembly on a surface, it is usually assumed that the Fermi level is located in the gap between the highest occupied molecular orbital (HOMO) and the lowest unoccupied molecular orbital (LUMO).

The work function depends on the surface considered. For example, in a tungsten crystal the WF depends on the crystallographic plane investigated as proven by the work function values of 4.63, 5.25 and 4.47 eV measured for the (100), (110) and (111) surfaces, respectively.[58] In the case of thin films, it has been demonstrated that the work function strongly depends on the *surface* of the material under study, which differs from its bulk electronic structure.[59] For KPFM measurements of films with a few layers thickness, the CPD is not simply given by the difference in work function since the contribution of the interfacial states has to be considered.[59] The contact potential is also known as surface potential (SP), which underlines one of the main features of KPFM: its surface sensitivity.

On the nanometric scale, the local variation of surface potential can be measured by KPFM; this methodology made it possible to visualize differences in local WF up to 250 meV between different crystallographic facets of small inorganic[60–63] and organic crystals.[64] In general, a given material can exhibit different SPs as determined by the structure at the atomic and molecular level as well as by the difference in charge carrier concentration. This has been proven by detecting a 40 meV difference in work function between amorphous and crystalline Ag–In–Sn–Te films used as rewritable compact disks,[65] or in the differences in SP (up to 400 meV) observed for different assemblies obtained from an alkylated polycyclic aromatic hydrocarbon.[66]

The influence of changes in the chemical structure of a surface, *i.e.* chemical functionalization, on its SP can be determined by KPFM.[67] For example, using SAMs chemisorbed on a metal electrode, it is possible to tune the WF of the surface. Kelvin probe measurements revealed a variation of WF from 3.8 to 5.5 eV obtained by adsorbing on a silver substrate either alkanethiols or perfluorinated alkanethiols, respectively. Similarly, the WF of gold can be varied between 4.1 and 5.5 eV, improving in this way the charge injection at gold–polymer[68] or gold–nanotube[69] interfaces. The WF of an ITO substrate can be modified by chemically functionalizing its surface with chlorosilanes,[70] acids or organic molecules,[71] or by physisorbing a doped polymer layer onto its surface.[72] The very high sensitivity of KPFM to the surface chemistry made it possible to map numerous processes such as the variation of the WF of a silicon substrate upon adsorption of a water layer from the humidity present in the air,[73,74] the corrosion phenomena in Al-based alloys on the microscopic scale,[75] and the *in-situ* operation of a chemical sensor of pyridine vapor.[76]

One key aspect that has to be taken into account when measuring the SP of ultra thin films by KPFM is the effective contribution of the substrate. Given that KPFM relies on long-range electrostatic interactions, the area of the surface interacting with the tip (and thus affecting the measured potential) can be expected to extend over several nanometers.[77] Since the characterization of the electronic properties of ultra-thin organic layers adsorbed on a solid substrate is of great interest, the removal of the contribution due to the

underlying macroscopic conductive substrate is of paramount importance. Because of this reason, the most significant, quantitative measurements are obtained on nano-patterned surfaces, where two or more types of molecular architectures are exposed on different areas of the same surface, so that differences observed are ascribable to the adsorbed molecule, and not to the substrate. The variation in surface potential between the different areas is used to bestow information on the adsorbate electrical dipole, chemical structure and density of packing, as detailed below.

Measuring the electronic potential of monomolecular thick self-assembled layers

Systematic measurements of the SP of self assembled monolayers (SAMs) have been performed by the groups of Sugimura and Saito.[78–83] In their studies, the silicon surface was functionalized with different types of silanes, and the SP measured by KPFM. Making use of mask patterning, the potential differences between SAMs of different molecules could be measured on the micron scale by direct KPFM visualization (Fig. 3).

The molecules had very different dipole moments and orientations, being based on either linear alkanes, or fluorinated alkanes, or molecules containing amino or chloride groups. KPFM measurements of the patterned surfaces clearly showed the differences in surface potential due to the different dipoles present in the SAM. By calculating the dipole moment using *ab-initio* methods and comparing it to the measured surface potential, it was possible to estimate the density of molecules adsorbed on the surface.[78]

The measured SP depends not only on the molecular dipole, but also on the length of the molecule forming the SAM, *i.e.* the thickness of the SAM. By adsorbing on the same substrate alkanes with different lengths, a clear increase of the potential with the number of CH_2 units was found, although differing values of SP increase of 9 mV per CH_2 unit[84] and 14 mV per CH_2 unit[85] were reported in two independent studies. In another experiment, by adsorbing an alkanethiol, *i.e.* $CH_3(CH_2)_9SH$, either perpendicular or flat on gold, SAMs with SP differences up to 150 mV were obtained.[86]

Due to the versatility and simplicity of KPFM, chemical modifications of SAMs could also be followed nearly in real time. The microscope tip can be employed to reversibly oxidize and reduce amino groups (NH_2) exposed on a SAM to nitroso (NO) moieties by simply inverting the SP,[83] forming lines and patterns on nanometric scales on the SAM (Fig. 4). Alternatively, the decomposition of an organosilane SAM can be induced by UV irradiation, and monitored with KPFM.[81,82]

On the macroscopic scale, Kelvin probe measurements make it possible also to map reversible reactions such as the

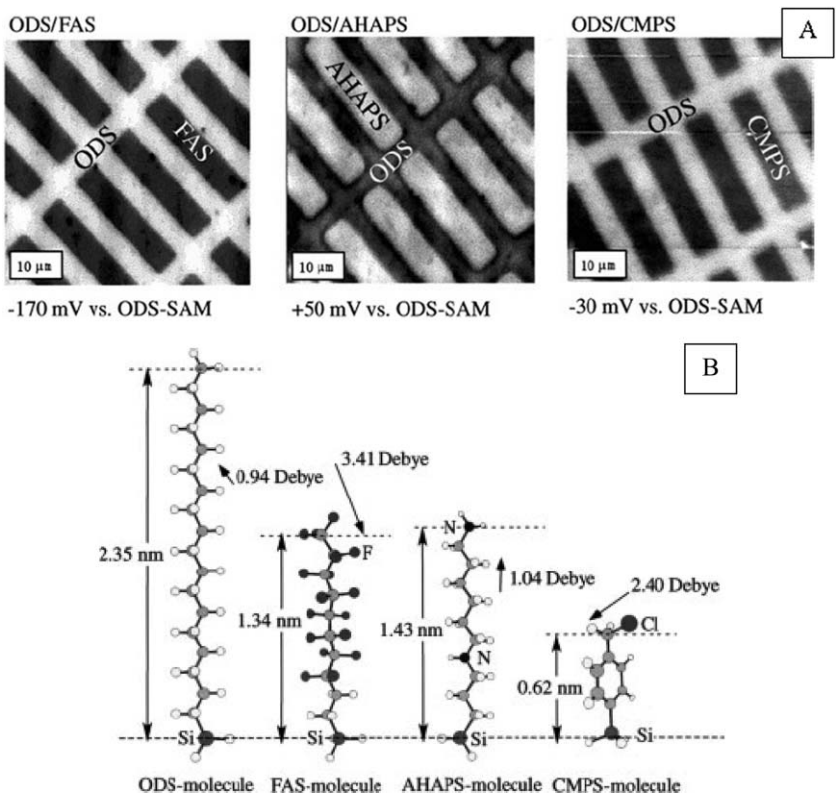

Fig. 3 (A) KPFM images of binary organosilane SAMs patterned by photolithography. These SAMs, terminated with different functional groups, were prepared on n-type silicon substrates by chemical vapor deposition from *n*-octadecyltrimethoxysilane (**ODS**: $H_3C(CH_2)_{17}Si(OCH_3)_3$), heptadecafluoro-1,1,2,2-tetrahydrodecyl-1-trimethoxysilane **FAS**: $F_3C(CF_2)_7(CH_2)_2Si(OCH_3)_3$), *n*-(6-aminohexyl)aminopropyltrimethoxysilane (**AHAPS**: $H_2N(CH_2)_6NH(CH_2)_3Si(OCH_3)_3$) and 4-(chloromethyl)phenyltrimethoxysilane (**CMPS**: $H_2ClC(C_6H_4)Si(OCH_3)_3$). (B) Molecular structures and dipole moments for the ODS, FAS, AHAPS and CMPS molecular models. Both images are reproduced with permission from ref 78, Copyright 2002, John Wiley & Sons, Ltd.

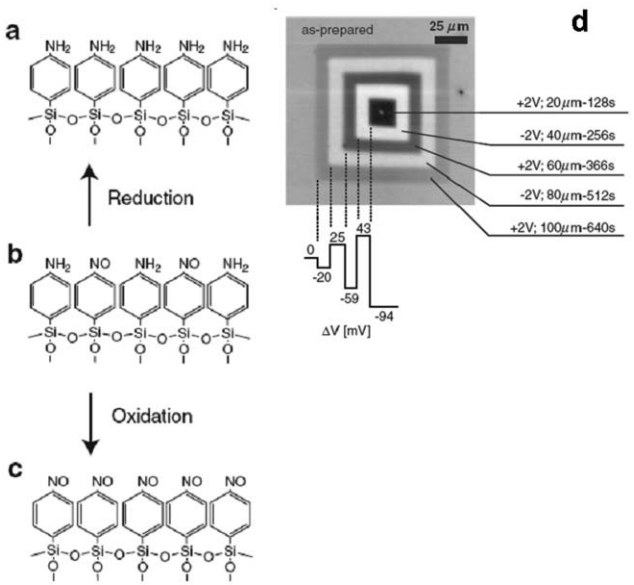

Fig. 4 Chemical structures of *p*-aminophenyltrimethoxysilane (APhS, $H_2N(C_6H_4)Si(OCH_3)_3$) SAM in (A) reduced, (B) partially oxidized and (C) oxidized states. (D) Multiple drawing on APhS-SAM. 100, 80, 60, 40 and 20 mm^2 square regions were oxidized or reduced, in that order, by AFM probe scanning at a bias voltage of −2 or +2 V, respectively, as indicated. A time for completing each square drawing is indicated as well. The graph at the lower left shows surface potential values of the probe scanned regions with respect to the potential of the un-scanned region, namely, the as-prepared region, on the APhS-SAM. Images reproduced with permission from ref. 83. Copyright 2004, The Japan Society of Applied Physics.

photo-isomerization of azobenzenes SAMs on gold,[87,88] and the complexation of bipyridine (PhBP) derivatives with palladium atoms on gold (Fig. 5).[89] The different contrast of the diverse self-assembled species is determined by their different electric dipole moments.

In the case of single component and thicker layers, differences in SP can be due to the presence of crystalline domains, which strongly affect the charge transport in the layer.[90] Even when no current is passing through the material, a SP difference is observed at grain boundaries in pentacene layers (Fig. 6).[91] The cause of this potential drop has been attributed to the selective adsorption of water and oxygen. In another experiment, high and low packing density phases of a LB film of hexa-*peri*-hexabenzocoronene molecules could clearly be distinguished by their different SP.[92]

Most interestingly, KPFM is a viable tool to explore dynamic properties of functional materials "in action", *i.e.* incorporated in a working device. The flat source–drain architecture of organic transistors can be suitably explored by the KPFM while the transistor is operating by monitoring the effect of different source and gate voltages.[93–98] A seminal work in this field has been reported by Bürgi *et al.*:[93] KPFM has been used to unveil the charge transport properties of the active polythiophene layer in a working transistor. In another set of experiments, KPFM was used to explore the density of states (DOS) of a molecular solid deposited as a thick film used in a transistor architecture. Sharp peaks and broadening of the DOS were observed in this system as a result of doping.[94] A limiting factor in organic transistors, which can be easily quantified with KPFM, is the presence of potential drops at

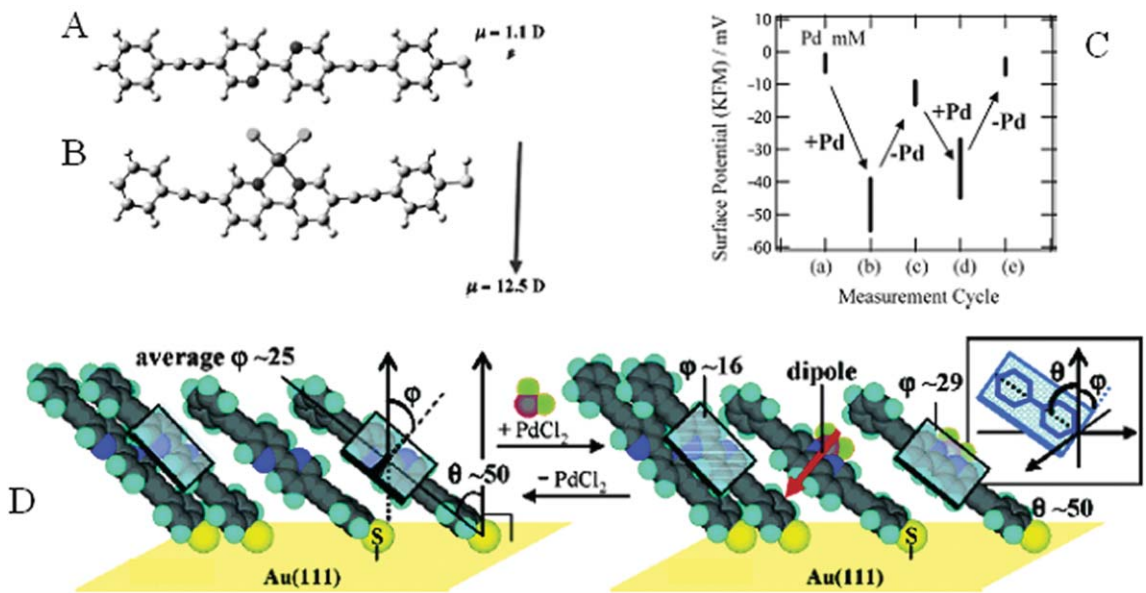

Fig. 5 Optimised structures of the PhBP derivatives. (A) PhBP thiol and (B) its complex with $PdCl_2$. Red arrows indicate electric dipole moments. (C) Surface potential variation during cycles of complexation and de-complexation in monolayers as measured by KPFM. (a) As prepared and (b) after coordinating with $PdCl_2$ (concentration: 3 mM) and rinsing. (c) After washing with ethylenediamine (EDA). (d) After coordinating again with $PdCl_2$ (concentration: 3 mM) and rinsing. (e) After washing again with EDA. (D) Schematic illustration for SAMs of PhBP on Au(111) in the de-complexed and complexed form. Grey arrow indicates a dipole moment induced in the PhBP–$PdCl_2$ complex. Inset illustrates the orientation of bipyridine ring to understand the tilt angles of θ and φ. The rectangle indicates the plane of the bipyridine ring. All images are reproduced with permission from ref. 89. Copyright 2006, American Chemical Society.

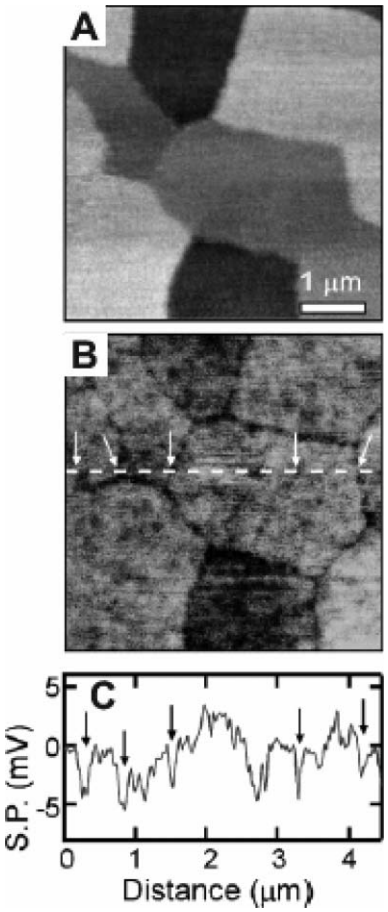

Fig. 6 (A) Lateral force microscopy and (B) surface potential maps of a small region of a pentacene monolayer on SiO_2, displaying potential wells at the grain boundaries. The corresponding topography image (not shown) is featureless. (C) Surface potential line section traced along the dashed line in (B). The arrows indicate the grain boundary potential wells. The measured depth of the wells averages between *ca.* −5 and −10 mV over several samples. Images reproduced with permission from ref. 91. Copyright 2006, Wiley–VCH.

the organic–metal interface.[96,97] In general, by measuring the potential decay in the source–drain gap, the conductivity of the material can be quantified.[93] The measured SP profile drop revealed a high resistance at the electrodes interface emerging as a potential drop.[97] Moreover the existence of high resistance within the layer due to domain boundaries in the 2D polycrystalline structure can be highlighted by the presence of steps in the SP decay along the transistor channel.[90] Furthermore, both the charge mobility and the DOS of the material can be measured by varying the voltage applied.[93,94] The presence of electrical traps (about 200 meV lower than the neighboring sites) can also be inferred by changes in the surface potential.[96] By and large, making use of a single technique it is possible to obtain an extensive characterization of many physical properties of the material used in the transistor.

An even more fascinating physical process which can be mapped by KPFM is the photovoltaic effect, in which charges are not injected from external electrodes but are generated directly in the material as a result of the absorption of photons. Also in this case, the material can be characterized directly when it is incorporated in real solar cells although, due to the vertical geometry of solar cells, the top electrode has to be removed to perform the KPFM measurement, thus the device can be studied only in the open circuit configuration. In this way, the generation of charges due to photovoltaic effect has been observed in different types of acceptor/donor organic blends including fullerene/PPV,[99] F8BT/PFB polyfluorenes,[100] *S*,*S*-dioxide oligothiophene/polythiophene (Fig. 7),[64] and TiO_2/phtalocyanine–perylene composite.[101]

A major limitation of KPFM is that it relies on long-range electrostatic interactions to map a surface, thus both its lateral and vertical resolution are lower than those obtained using other SPM based techniques. For this reason, the charge transfer in photovoltaic blends can be observed only when the two materials composing the blend are phase-separated on the tens of nanometers scale. An increase in lateral resolution can be achieved by decreasing the tip–sample distance, although the induced polarization on the sample surface then prevents a direct and quantitative measurement of the work function. Albeit quantitative measurements on nanometric scale are difficult, nano-objects having different potential can anyhow be qualitatively resolved by KPFM, and in some cases the effective potential can be estimated by modeling of the experimental KPFM data.[77]

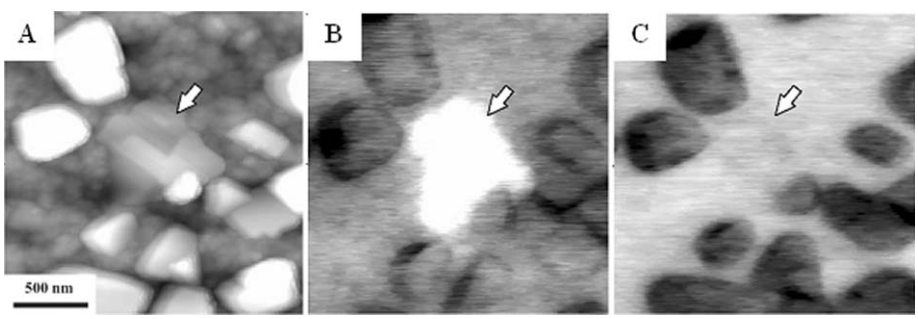

Fig. 7 (A) Topographical image of a blend of *S*,*S*-dioxide oligothiophene and polythiophene acting as electron acceptor and donor, respectively, and (B) surface potential images of the same region recorded (B) in the dark and (C) under illumination (61 mW cm^{-2}). While the acceptor crystals become negatively charged upon light irradiation (dark contrast), the amorphous polymeric matrix becomes positively charged. The arrows indicate a polymeric crystalline domain that upon light irradiation becomes positively charged, *i.e.* it becomes electronically leveled to the amorphous matrix. *Z*-scale: (A) 207 nm, (B) 167 mV and (C) 158 mV. Images reproduced with permission from ref 64. Copyright 2007, Wiley–VCH.

Measuring the potential of biological molecules

A very attractive yet still poorly explored field of application of the KPFM technique is the measurement of the electric potential of biological molecules such as proteins.

KPFM experiments have been performed on PS I, a chlorophyll dimer existing in many green plants, responsible for their photosynthetic activity. This robust supramolecular system can be extracted, immobilized on a substrate and visualized by SPM. The changes in potential due to illumination can be visualized with good lateral resolution by KPFM and thus the reaction centre of PS I responsible for the photosynthetic activity can be localized into the supramolecular structure.[102,103] Another application of KPFM on biological systems involved bacteriorhodopsin, a 248 amino acid integral membrane protein found in the purple membrane of *Halobacterium salinarum*. It acts as a light-to-chemical energy transducer by pumping protons across the cell membrane in response to sunlight. Making use of a modified KPFM, the photoinduced surface potential change of bacteriorhodopsin was measured at different pH values, allowing the study of the mechanism of photocharge generation on the external side of the *Halobacterium* cellular membrane.[104] The same membrane was studied by KPFM by Knapp *et al.*, who were able to deposit planar fragments of the *Halobacterium* cellular membrane on graphite and to measure their potential under a controlled humidity atmosphere. The membrane lied on the graphite exposing either one of its two different faces (cytoplasmic face and extracellular face), which could be then distinguished on the basis of their different roughness and their surface potential (Fig. 8).[105]

Conclusions and outlook

In this Feature Article we have introduced and discussed different AFM based approaches to study electrical and electronic properties of nanoscale structural motifs under ambient conditions, as a valuable alternative to measurements performed under more expensive and technologically less relevant ultra-high vacuum environments. The direct information provided by these techniques is fundamental for the optimization of functional materials and opens up a large range of nanoscale applications.

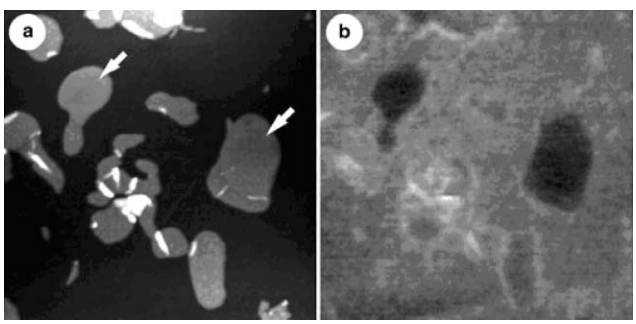

Fig. 8 (a) Topographic and (b) surface potential images of a *Halobacterium* cellular membrane adsorbed on mica recorded in the darkness and at 64% relative humidity. The surface exhibits smooth (arrows) and rough patches. The images are 5.5 μm × 5.5 μm with a gray scale of (a) 18 nm and (b) 70 mV. Both images are reproduced with permission from ref. 105. Copyright 2002, John Wiley & Sons, Ltd.

One major challenge in the field is the improvement of spatial resolution for all the modes presented above. In this context, improvements can be pursued by fabrication of sharper tips for better resolution, or enhanced electronics (*e.g.* faster scanning) or new detection modes. It is also important to develop models and viable computational procedures to extrapolate quantitative information on properties down to a 1–10 nm scale. Furthermore, in both C-AFM and KPFM, controlled gas atmospheres can be employed to avoid the influence of water vapor adsorbed on the surface.

Through real-time mapping of the electrical and electronic characteristics of complex systems, AFM based approaches can be employed in the future to unravel supramolecular reactions and phenomena occurring at various interfaces, including assembly–disassembly processes, the switching between different self-assembled motifs controlled by external stimuli, and the self-healing of supramolecular arrangements. The combination with AFM imaging does not only open the routes towards the comparison of the electrical or electronic properties with the surface topography, but it also paves the way towards the simultaneous use of nanoscale characterization of the mechanical properties of molecular species, such as single molecule-based multichromophoric arrays.[106,107] The time evolution of the electric potential can also provide important information on dynamical processes, especially if used with stimuli modulated in time.[108] One can also envision future SPM-based electrical measurements performed at high speed, where the time resolution limit is given by contact quality (in the case of C-AFM) and by tip oscillation dynamics for KPFM.

Nanoscale electrical and electronic characterization of functional materials is still in its infancy. New developments can be foreseen and will be strictly related to the fabrication of more and more complex systems whose dynamic properties can be unveiled also under the effect of different external stimuli, *e.g.* light irradiation. Achieving a full control over the properties of supramolecularly engineered functional materials will represent a milestone in the development of the emerging field of nanochemistry and nanoscale science. In particular AFM based methodologies can be fundamental in the years to come to research activity at the interface between biology and nanotechnology, paving the way towards the design and fabrication of artificial biohybrid machines.

Finally, unraveling the nanoworld is not only fascinating by itself, but it opens interesting perspectives for nanotechnological applications, in particular in the fields of molecular (opto)electronics, catalysis, sensors, and nanomedicine.

Acknowledgements

This work was supported by the EU Marie Curie through the EST project SUPER (MEST-CT-2004-008128) as well as the RTN projects PRAIRIES (MRTN-CT-2006-035810) and THREADMILL (MRTN-CT-2006-036040), the ERA-Chemistry project SurConFold, the ESF-SONS2-SUPRAMATES project, the Regione Emilia-Romagna PRIITT Nanofaber Net-Lab and the EU-ForceTool

(NMP4-CT-2004-013684) project. M. S. is Chargé de Recherches of the FNRS (Belgium).

References

1 Special Issue, *Science*, 2002, **295**, 2395.
2 A. Schenning and E. W. Meijer, *Chem. Commun.*, 2005, 3245.
3 Special Issue, *Adv. Mater.*, 2006, **18**, 1227.
4 P. Mulvaney, *MRS Bull.*, 2001, **26**, 1009.
5 F. J. M. Hoeben, P. Jonkheijm, E. W. Meijer and A. Schenning, *Chem. Rev.*, 2005, **105**, 1491.
6 M. Van der Auweraer and F. C. De Schryver, *Nat. Mater.*, 2004, **3**, 507.
7 A. Janshoff, M. Neitzert, Y. Oberdörfer and H. Fuchs, *Angew. Chem., Int. Ed.*, 2000, **39**, 3213.
8 P. Samorì, *J. Mater. Chem.*, 2004, **14**, 1353.
9 P. Samorì, *Scanning Probe Microscopies: beyond imaging – Manipulation of Molecules and Nanostructures*, WILEY–VCH Verlag GmbH & Co. KGaA, Weinheim, 2006, Weinheim, 2006.
10 D. C. Coffey and D. S. Ginger, *Nat. Mater.*, 2006, **5**, 735.
11 P. Samorì, *Chem. Soc. Rev.*, 2005, **34**, 551.
12 S. S. Sheiko and M. Möller, *Chem. Rev.*, 2001, **101**, 4099.
13 H. Takano, J. R. Kenseth, S.-S. Wong, J. C. O'Brien and M. D. Porter, *Chem. Rev.*, 1999, **99**, 2845.
14 C. Bustamante, J. F. Marko, E. D. Siggia and S. Smith, *Science*, 1994, **265**, 1599.
15 E. L. Florin, V. T. Moy and H. E. Gaub, *Science*, 1994, **264**, 415.
16 C. D. Frisbie, L. F. Rozsnyai, A. Noy, M. S. Wrighton and C. M. Lieber, *Science*, 1994, **265**, 2071.
17 M. Nonnenmacher, M. P. O'Boyle and H. K. Wickramasinghe, *Appl. Phys. Lett.*, 1991, **58**, 2921.
18 Q. Zhong, D. Innis, K. Kjoller and V. B. Elings, *Surf. Sci. Lett.*, 1993, **290**, L688.
19 Y. Martin and H. K. Wickramasinghe, *Appl. Phys. Lett.*, 1987, **50**, 1455.
20 A. RosaZeiser, E. Weilandt, S. Hild and O. Marti, *Meas. Sci. Technol.*, 1997, **8**, 1333.
21 R. E. Holmlin, R. Haag, M. L. Chabinyc, R. F. Ismagilov, A. E. Cohen, A. Terfort, M. A. Rampi and G. M. Whitesides, *J. Am. Chem. Soc.*, 2001, **123**, 5075.
22 C. Zhou, M. R. Deshpande, M. A. Reed, L. Jones and J. M. Tour, *Appl. Phys. Lett.*, 1997, **71**, 611.
23 M. A. Reed, C. Zhou, C. J. Muller, T. P. Burgin and J. M. Tour, *Science*, 1997, **278**, 252.
24 A. Bezryadin, C. Dekker and G. Schmid, *Appl. Phys. Lett.*, 1997, **71**, 1273.
25 T. Dadosh, Y. Gordin, R. Krahne, I. Khivrich, D. Mahalu, V. Frydman, J. Sperling, A. Yacoby and I. Bar-Joseph, *Nature*, 2005, **436**, 677.
26 N. Jeong-Seok, A. Jennifer, K. L. Chandra, C. Chu, C. B. Gorman and G. N. Parsons, *Nanotechnology*, 2007, **18**, 035203.
27 J. N. Nxumalo, D. T. Shimizu and D. J. Thomson, *J. Vac. Sci. Technol., B*, 1996, **14**, 386.
28 H. Dai, E. Wong and C. M. Lieber, *Science*, 1996, **272**, 523.
29 D. L. Klein and P. L. McEuen, *Appl. Phys. Lett.*, 1995, **66**, 2478.
30 S. J. O'Shea, R. M. Atta, M. P. Murrell and M. E. Welland, *J. Vac. Sci. Technol., B*, 1995, **13**, 1945.
31 T. W. Kelley, E. L. Granstrom and C. D. Frisbie, *Adv. Mater.*, 1999, **11**, 261.
32 A. Salomon, D. Cahen, S. Lindsay, J. Tomfohr, V. B. Engelkes and C. D. Frisbie, *Adv. Mater.*, 2003, **15**, 1881.
33 C. Gomez-Navarro, P. J. De Pablo, J. Gomez-Herrero, B. Biel, F. J. Garcia-Vidal, A. Rubio and F. Flores, *Nat. Mater.*, 2005, **4**, 534.
34 M. J. Loiacono, E. L. Granstrom and C. D. Frisbie, *J. Phys. Chem. B*, 1998, **102**, 1679.
35 T. Hassenkam, K. Moth-Poulsen, N. Stuhr-Hansen, K. Norgaard, M. S. Kabir and T. Bjornholm, *Nano Lett.*, 2004, **4**, 19.
36 T. W. Kelley and C. D. Frisbie, *J. Phys. Chem. B*, 2001, **105**, 4538.
37 M. Nakamura, H. Yanagisawa, S. Kuratani, M. Iizuka and K. Kudo, *Thin Solid Films*, 2003, **438**, 360.
38 E. M. Muller and J. A. Marohn, *Adv. Mater.*, 2005, **17**, 1410.
39 M. Surin, S. Cho, J. D. Yuen, G. Wang, K. Lee, P. Leclère, R. Lazzaroni, D. Moses and A. J. Heeger, *J. Appl. Phys.*, 2006, **100**, 33712.
40 Y. Xia, J. A. Rogers, K. E. Paul and G. M. Whitesides, *Chem. Rev.*, 1999, **99**, 1823.
41 M. A. Rampi and G. M. Whitesides, *Chem. Phys.*, 2002, **281**, 373.
42 S. Wakamatsu, U. Akiba and M. Fujihira, *Jpn. J. Appl. Phys., Part 1*, 2002, **41**, 4998.
43 D. J. Wold and C. D. Frisbie, *J. Am. Chem. Soc.*, 2001, **123**, 5549.
44 B. Xu and N. J. Tao, *Science*, 2003, **301**, 1221.
45 X. D. Cui, A. Primak, X. Zarate, J. Tomfohr, O. F. Sankey, A. L. Moore, T. A. Moore, D. Gust, G. Harris and S. M. Lindsay, *Science*, 2001, **294**, 571.
46 G. Leatherman, E. N. Durantini, D. Gust, T. A. Moore, A. L. Moore, S. Stone, Z. Zhou, P. Rez, Y. Z. Liu and S. M. Lindsay, *J. Phys. Chem. B*, 1999, **103**, 4006.
47 I.-W. P. Chen, M.-D. Fu, W.-H. Tseng, J.-Y. Yu, S.-H. Wu, C.-J. Ku, C.-h. Chen and S.-M. Peng, *Angew. Chem., Int. Ed.*, 2006, **45**, 5814.
48 J. W. Zhao, J. J. Davis, M. S. P. Sansom and A. Hung, *J. Am. Chem. Soc.*, 2004, **126**, 5601.
49 H. Cohen, C. Nogues, D. Ullien, S. Daube, R. Naaman and D. Porath, *Faraday Discuss.*, 2006, **131**, 367.
50 C. Gomez-Navarro, F. Moreno-Herrero, P. J. de Pablo, J. Colchero, J. Gomez-Herrero and A. M. Baro, *Proc. Natl. Acad. Sci. USA*, 2002, **99**, 8484.
51 R. Thomson and J. Moreland, *J. Vac. Sci. Technol., B*, 1995, **13**, 1123.
52 V. B. Engelkes, J. M. Beebe and C. D. Frisbie, *J. Phys. Chem. B*, 2005, **109**, 16801.
53 X. D. Cui, X. Zarate, J. Tomfohr, A. Primak, A. L. Moore, T. A. Moore, D. Gust, G. Harris, O. F. Sankey and S. M. Lindsay, *Ultramicroscopy*, 2002, **92**, 67.
54 A. V. Tivanski, J. E. Bemis, B. B. Akhremitchev, H. Y. Liu and G. C. Walker, *Langmuir*, 2003, **19**, 1929.
55 V. Palermo, M. Palma and P. Samorì, *Adv. Mater.*, 2006, **18**, 145.
56 M. Fujihira, *Annu. Rev. Mater. Sci.*, 1999, **29**, 353.
57 M. Prutton, *Introduction to Surface Physics*, Oxford University Press, Oxford, 1994.
58 R. A. Strayer, W. Mackie and L. W. Swanson, *Surf. Sci.*, 1973, **34**, 225.
59 H. Ishii, N. Hayashi, E. Ito, Y. Washizu, K. Sugi, Y. Kimura, M. Niwano, Y. Ouchi and K. Seki, *Phys. Status Solidi A*, 2004, **201**, 1075.
60 S. Sadewasser, T. Glatzel, M. Rusu, A. Jager-Waldau and M. C. Lux-Steiner, *Appl. Phys. Lett.*, 2002, **80**, 2979.
61 S. Sadewasser, T. Glatzel, S. Schuler, S. Nishiwaki, R. Kaigawa and M. C. Lux-Steiner, *Thin Solid Films*, 2003, **431**, 257.
62 J. Zuniga-Perez, V. Munoz-Sanjose, E. Palacios-Lidon and J. Colchero, *Phys. Rev. Lett.*, 2005, **95**, 226105.
63 N. Gaillard, M. Gros-Jean, D. Mariolle, F. Bertin and A. Bsiesy, *Appl. Phys. Lett.*, 2006, **89**, 154101.
64 V. Palermo, G. Ridolfi, A. M. Talarico, L. Favaretto, G. Barbarella, N. Camaioni and P. Samorí, *Adv. Funct. Mater.*, 2007, **17**, 472.
65 T. Nishimura, M. Iyoki and S. Sadayama, *Ultramicroscopy*, 2002, **91**, 119.
66 V. Palermo, M. Palma, Z. Tomovic, M. D. Watson, R. Friedlein, K. Müllen and P. Samorì, *ChemPhysChem*, 2005, **6**, 2371.
67 R. Sfez, N. Peor, S. R. Cohen, H. Cohen and S. Yitzchaik, *J. Mater. Chem.*, 2006, **16**, 4044.
68 B. de Boer, A. Hadipour, M. M. Mandoc, T. van Woudenbergh and P. W. M. Blom, *Adv. Mater.*, 2005, **17**, 621.
69 X. D. Cui, M. Freitag, R. Martel, L. Brus and P. Avouris, *Nano Lett.*, 2003, **3**, 783.
70 R. A. Hatton, S. R. Day, M. A. Chesters and M. R. Willis, *Thin Solid Films*, 2001, **394**, 292.
71 B. Johnev, M. Vogel, K. Fostiropoulos, B. Mertesacker, M. Rusu, M. C. Lux-Steiner and A. Weidinger, *Thin Solid Films*, 2005, **488**, 270.
72 H. Frohne, C. R. McNeill, G. G. Wallace and P. C. Dastoor, *J. Phys. D: Appl. Phys.*, 2004, **37**, 165.
73 H. Sugimura, Y. Ishida, K. Hayashi, O. Takai and N. Nakagiri, *Appl. Phys. Lett.*, 2002, **80**, 1459.

74 N. Nakagiri, H. Sugimura, Y. Ishida, K. Hayashi and O. Takai, *Surf. Sci.*, 2003, **532**, 999.
75 T. H. Muster and A. E. Hughes, *J. Electrochem. Soc.*, 2006, **153**, B474.
76 R. Grover, B. M. Carthy, Y. Zhao, G. E. Jabbour, D. Sarid, G. M. Laws, B. R. Takulapalli, T. J. Thornton and D. Gust, *Appl. Phys. Lett.*, 2004, **85**, 3926.
77 A. Liscio, V. Palermo, D. Gentilini, F. Nolde, K. Müllen and P. Samorì, *Adv. Funct. Mater.*, 2006, **16**, 1407.
78 N. Saito, K. Hayashi, H. Sugimura, O. Takai and N. Nakagiri, *Surf. Interface Anal.*, 2002, **34**, 601.
79 K. Hayashi, N. Saito, H. Sugimura, O. Takai and N. Nakagiri, *Langmuir*, 2002, **18**, 7469.
80 H. Sugimura, K. Hayashi, N. Saito, N. Nakagiri and O. Takai, *Appl. Surf. Sci.*, 2002, **188**, 403.
81 H. Sugimura, N. Saito, Y. Ishida, I. Ikeda, K. Hayashi and O. Takai, *J. Vac. Sci. Technol., A*, 2004, **22**, 1428.
82 H. Sugimura, N. Saito, N. Maeda, I. Ikeda, Y. Ishida, K. Hayashi, L. Hong and O. Takai, *Nanotechnology*, 2004, **15**, S69.
83 H. Sugimura, *Jpn. J. Appl. Phys., Part 1*, 2004, **43**, 4477.
84 T. Ichii, T. Fukuma, K. Kobayashi, H. Yamada and K. Matsushige, *Nanotechnology*, 2004, **15**, S30.
85 J. Lu, E. Delamarche, L. Eng, R. Bennewitz, E. Meyer and H. J. Guntherodt, *Langmuir*, 1999, **15**, 8184.
86 T. Ichii, T. Fukuma, K. Kobayashi, H. Yamada and K. Matsushige, *Appl. Surf. Sci.*, 2003, **210**, 99.
87 D. Gustina, E. Markava, I. Muzikante, B. Stiller and L. Brehmer, *Adv. Mater. Opt. Electron.*, 1999, **9**, 245.
88 B. Stiller, G. Knochenhauer, E. Markava, D. Gustina, I. Muzikante, P. Karageorgiev and L. Brehmer, *Mater. Sci. Eng., C*, 1999, **8–9**, 385.
89 T. Nakamura, E. Koyama, Y. Shimoi, S. Abe, T. Ishida, K. Tsukagoshi, W. Mizutani, H. Tokuhisa, M. Kanesato, I. Nakai, H. Kondoh and T. Ohta, *J. Phys. Chem. B*, 2006, **110**, 9195.
90 T. Hassenkam, D. R. Greve and T. Bjornholm, *Adv. Mater.*, 2001, **13**, 631.
91 K. Puntambekar, J. P. Dong, G. Haugstad and C. D. Frisbie, *Adv. Funct. Mater.*, 2006, **16**, 879.
92 N. Reitzel, T. Hassenkam, K. Balashev, T. R. Jensen, P. B. Howes, K. Kjaer, A. Fechtenkotter, N. Tchebotareva, S. Ito, K. Müllen and T. Bjornholm, *Chem. Eur. J.*, 2001, **7**, 4894.
93 L. Bürgi, H. Sirringhaus and R. H. Friend, *Appl. Phys. Lett.*, 2002, **80**, 2913.
94 O. Tal, Y. Rosenwaks, Y. Preezant, N. Tessler, C. K. Chan and A. Kahn, *Phys. Rev. Lett.*, 2005, **95**, 256405.
95 L. Bürgi, R. H. Friend and H. Sirringhaus, *Appl. Phys. Lett.*, 2003, **82**, 1482.
96 L. Bürgi, T. Richards, M. Chiesa, R. H. Friend and H. Sirringhaus, *Synth. Met.*, 2004, **146**, 297.
97 K. P. Puntambekar, P. V. Pesavento and C. D. Frisbie, *Appl. Phys. Lett.*, 2003, **83**, 5539.
98 J. A. Nichols, D. J. Gundlach and T. N. Jackson, *Appl. Phys. Lett.*, 2003, **83**, 2366.
99 H. Hoppe, T. Glatzel, M. Niggemann, A. Hinsch, M. C. Lux-Steiner and N. S. Sariciftci, *Nano Lett.*, 2005, **5**, 269.
100 M. Chiesa, L. Bürgi, J. S. Kim, R. Shikler, R. H. Friend and H. Sirringhaus, *Nano Lett.*, 2005, **5**, 559.
101 J. Cao, J. Z. Sun, J. Hong, X. G. Yang, H. Z. Chen and M. Wang, *Appl. Phys. Lett.*, 2003, **83**, 1896.
102 I. Lee, B. L. Justus, J. W. Lee and E. Greenbaum, *J. Phys. Chem. B*, 2003, **107**, 14225.
103 I. Lee, J. W. Lee, A. Stubna and E. Greenbaum, *J. Phys. Chem. B*, 2000, **104**, 2439.
104 I. Lee, E. Greenbaum, S. Budy, J. R. Hillebrecht, R. R. Birge and J. A. Stuart, *J. Phys. Chem. B*, 2006, **110**, 10982.
105 H. F. Knapp, P. Mesquida and A. Stemmer, *Surf. Interface Anal.*, 2002, **33**, 108.
106 P. Samorì, C. Ecker, I. Gössl, P. A. J. de Witte, J. J. L. M. Cornelissen, G. A. Metselaar, M. B. J. Otten, A. E. Rowan, R. J. M. Nolte and J. P. Rabe, *Macromolecules*, 2002, **35**, 5290.
107 J. Hernando, P. A. J. de Witte, E. van Dijk, J. Korterik, R. J. M. Nolte, A. E. Rowan, M. F. Garcia-Parajo and N. F. van Hulst, *Angew. Chem., Int. Ed.*, 2004, **43**, 4045.
108 C. Loppacher, U. Zerweck, S. Teich, E. Beyreuther, T. Otto, S. Grafstrom and L. M. Eng, *Nanotechnology*, 2005, **16**, S1.